Appl. Phys. A (2017) 123:321
DOI 10.1007/s00339-017-0757-0

Applied Physics A
Materials Science & Processing

Dynamic crushing behavior of open-cell aluminum foam with negative Poisson's ratio

Peiwen Zhang[1,2] · Zhihua Wang[1] · Longmao Zhao[1,2]

Received: 28 August 2016 / Accepted: 1 January 2017 / Published online: 7 April 2017

Abstract The dynamic crushing behavior of the open-cell aluminum foam with negative Poisson's ratio (NPR) was investigated using the finite-element (FE) method. The plateau stress, the specific energy absorption, and the deformation modes are determined using the FE models. The results indicate that the plateau stress and specific energy absorption (SEA) of NPR open-cell foam under impact loading are less than the conventional foam with the same relative density, and the deformation pattern of NPR open-cell foam material is completely different from the conventional foam material. The NPR open-cell foam material is not suitable for energy absorption under low-velocity impact, but the negative Poisson's ratio effect on deformation modes becomes smaller with the impact velocity increasing. The length-to-height ratio which is defined for a cell having certain geometric characteristics is a key parameter to design the NPR foams materials.

1 Introduction

Metal foams, due to their characteristic cellular microstructures, have many distinguished properties, such as a high specific stiffness/strength and the excellent capability of absorbing a large amount of energy by large plastic deformation [1], which are, therefore, easily available to be used as an core material of sandwich structures (beams and panels) in many protective engineering applications [2, 3]. As described by Gibson et al. [4] and Ashby et al. [5], the quasi-static mechanical performances, such as the compressive strength, elastic modulus, and stress–strain response, have widely been discussed. By varying the micro-scale parameters (e.g., through cell wall and face thickness, and area moments of inertia) of foam, the local load bearing capacity becomes a controllable spatial variable rather than an approximately constant value [6]. As we all know, most of sandwich structures and materials in nature as well as those manufactured by man have a cell structure with interior angles that are convex and result in the structure with a positive Poisson's ratio (PPR) which means that when stretched longitudinally, they become shorter in the lateral directions. Here, these cellular materials are referred to as the "conventional" materials. In contrast, for the reason of rarity of materials with NPR, the researchers have shown significant interest in finding such materials. Some cellular materials with the concave cell-wall angles are commonly called reentrant structures, which exhibit to achieve unusual properties, such as NPR and controllable instability of structures. Negative Poisson's ratio materials are also of great interest, because they typically have enhanced toughness and shear resistance, along with enhanced sound and vibration absorption. For example, negative Poisson's ratio has been exploited to manipulate wave propagation in reentrant cellular structures [4, 7, 8]. In addition, it has been exploited in fields as varied as medicine [9], fasteners [10], tougher composites [11], tissue engineering [12], national security and defense, i.e., for bulletproof vests and armor enhancement [13], and many other potential applications [14–16]. While bulk materials with engineered micro-structure have been the focus for generating materials exhibiting a negative Poisson's ratio, this is not

✉ Zhihua Wang
wangzh@tyut.edu.cn

[1] Institute of Applied Mechanics and Biomedical Engineering, Taiyuan University of Technology, Taiyuan 030024, China

[2] Shanxi Key Laboratory of Material Strength and Structural Impact, Taiyuan University of Technology, Taiyuan 030024, China

a requirement for the phenomenon to occur. These cellular materials have attracted more and more attention as a type of metamaterials. Therefore, how to establish the relations between micro-cell structures and the crushing response performance, and further realize the self design of reentrant cellular structures according to applicable demands, is always the frontier.

In this study, we adopt reentrant structures as a building block of mechanical metamaterials to achieve simultaneous negative Poisson's effect. Due to the high uniformity of the internal topologies (as shown in Figs. 1, 2), NPR open-cell foam is studied for improving the properties of low-density metal materials, and is notably preferential in dynamic machine parts for their good flexibility and shock absorption compared to heavier aluminum alloy parts. Further improvement and optimization of their energy absorption capacity is always the target.

2 FE model

2.1 Modeling geometry

In this study, the open-cell foams were all evolved from the planar reentrant structures which were combined with straight and sloping bar, forming a grid structure. The numerical model was made using the non-linear, explicit finite-element code LS-DYNA 3D. The FE model is shown in Fig. 1. In this study, three different types of foams with varying bar lengths which result in different relative densities were used in the compression tests. The bar length (l) and the interior angle (α) for all unit cells are 0.95 mm and 76°, but the height (h) are 1, 0.75 and 0.5 mm, respectively. The relative density of foams can be calculated by the following:

$$\bar{\rho} = \frac{\rho^*}{\rho_s} = \sum_{i=1}^{N} A_i l_i / V_0 \tag{1}$$

where A_i is the area of the ith bar, l_i is the ith bar length, and N is the amount of bars in the whole cubic with the

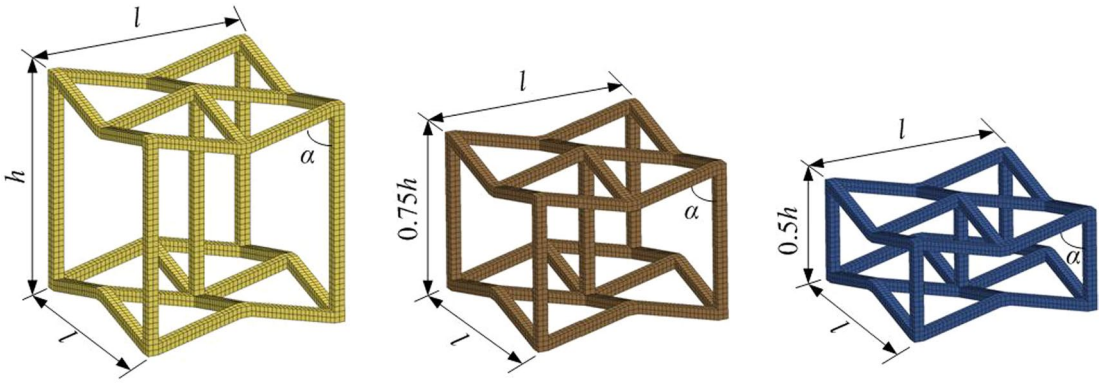

Fig. 1 FE model of three different unit cells

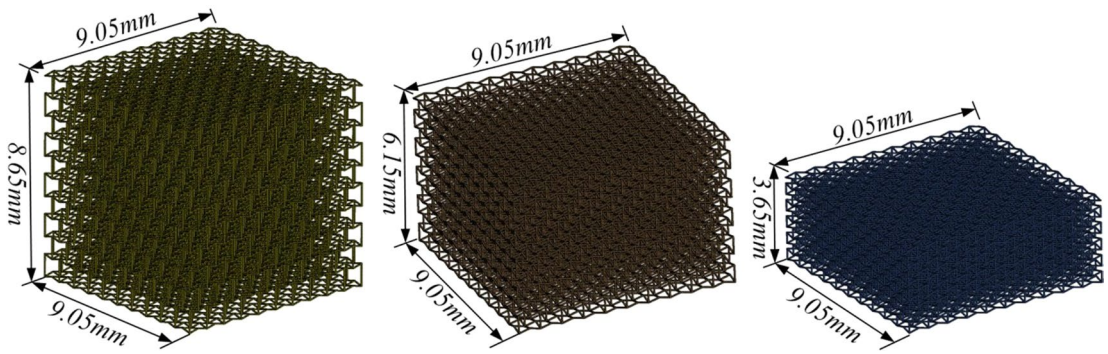

Fig. 2 The FE model sketch of three types of NPR foams

original volume of V_0. In this study, the relative density ($\bar{\rho}$) of cubic metal foam is 2.09, 2.67, and 4.03%, respectively.

The in-plane dimensions of all specimens used in simulations are 9.1×9.1 mm. Such dimensions ensure that each specimen has sufficient cells, so that the specimen-size effect is minimized and the measured properties can represent the bulk properties. Xu et al. [17] pointed out that the minimum number of cells for such HEXCEL honeycombs should be 9×9. Therefore, in this study, the number of cells in each specimen under the dynamic impact is 10×10×10, as shown in Fig. 2.

3 Modeling material

The mechanical behavior of NPR foam is represented by the bilinear strain-hardening model (see also the literature [18]). Since most aluminum alloys are strain rate insensitive, the effect of strain effect is ignored in the simulation. The rigid material is defined for the impact and supporting plates. The detail parameters of the material are listed in Table 1.

3.1 Boundary and initial conditions

The penalty function contact method is used to interpret the interaction between the plates and foams. The contact of automatic surface to surface is defined between the impact plate and NPR metallic foam, as well as between the NPR metallic foam and supporting plate. There may be some analogous contact between the bars of open-cell foam after deformation, so the contact of auto single surface is adopted; at the same time, the friction between the interfaces was not considered. The supporting plate is wholly fixed; meanwhile, the impact plate was given an initial velocity varied from 10 to 150 m/s. Here, the nominal compressive stress σ is defined as the ratio of the contact force, which on the contact area between the impact plate and NPR metallic foam, to the initial cross section areas of the model. The nominal strain ε is defined as the ratio of the overall compression of the model to its original length along the compression direction. Therefore, a dynamic compressive stress–strain curve could be obtained.

Table 1 Matrix material parameters of the NPR foam

Material	Young's modulus	Yield stress	Hardening modulus	Poisson's ratio	Density
Aluminum	68.97GPa	76 MPa	700 MPa	0.35	2700Kg/m3

4 Simulation results and discussion

4.1 Stress−strain response

The stress–strain curves of the NPR metallic foam with a same relative density 4.03% under different impact velocities are plotted in Fig. 3. It can be seen from Fig. 3a that the slope of curves is almost the same with each other before the stress reaches the peak stress at proximal end which is due to the same materials Young's module. When the curves exceed the peak stress, the stress of all curves drops to the plateau stress and then increases to the plateau stress with the strain increasing. At the proximal end, the plateau stress has an obvious increase with the impact velocities increasing. It indicates that the plateau stress is sensitive to loading rate. The crushing stress at the distal end was different from that at the impact side, as shown in Fig. 3b. It could be concluded that the plateau stress at the distal end is almost the same with others in spite of the impact velocities; meanwhile, it is clearly discovered from Fig. 3b

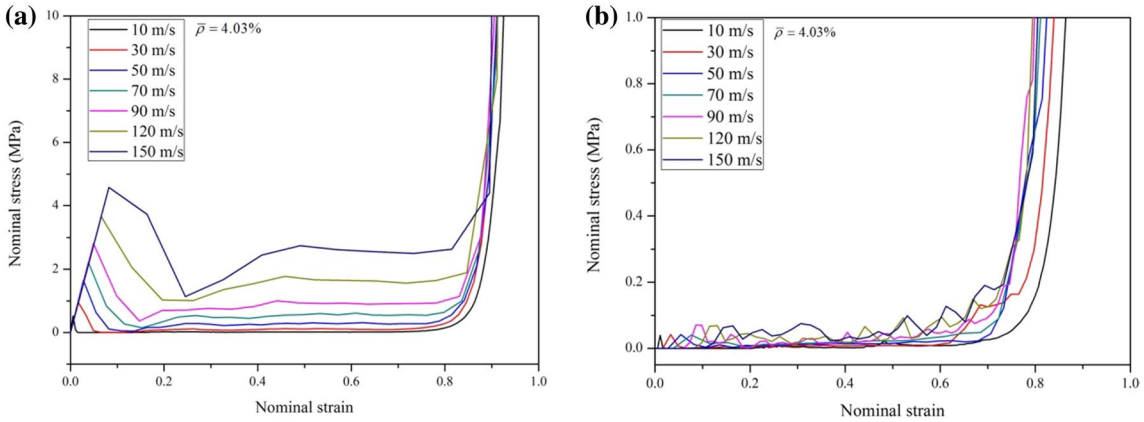

Fig. 3 Nominal stress–strain *curves* at proximal and distal ends of NPR metallic foam. **a** Proximal end; and **b** distal end

that the plateau stress is lower than that of proximal ends at higher loading speed. Based on the numerical consequence, there is, indeed, a potential imbalance between loading and supporting forces under high impact velocities. This imbalance between loading and supporting forces is also observed the same of many experiments and simulations [19, 20]. What is worth noting that there is a non-stress stage around the nominal strain 0.1 on the present nominal stress–strain curve as shown in Fig. 4. The previous studies [21, 22] show that the reflection-induced transient separation between foam and rigid plate can cause drastic stress drop in a very small strain range. The trend of present model curve is similar to the result of [23], but different from that of [24]. The reasonable explanation is that there is a temporary separation between the impact plate and the NPR foam due to the bending, torsion, and buckling of cell ribs, as shown in Fig. 5. And the structural softening is also another reason for this phenomenon. Under low impact velocities, the deformation is initially localized in one or two bands of collapsing cells, which may be the weakest regions of the sample, and then, the crushing bands diffuse until all are fully densified according to the numerical consequence. When impact speed increases, the crushing bands are highly localized at the impact side, which is the progressive deformation mode in usual, and then propagate along the impact direction. Hence, the loading stress level is overall enhanced due to increased inertial force and thus the zero-stress disappears at higher impact speeds. Thus, it needs to pay particular attention to this phenomenon for designer because of the non-load-carrying capacity of the structure.

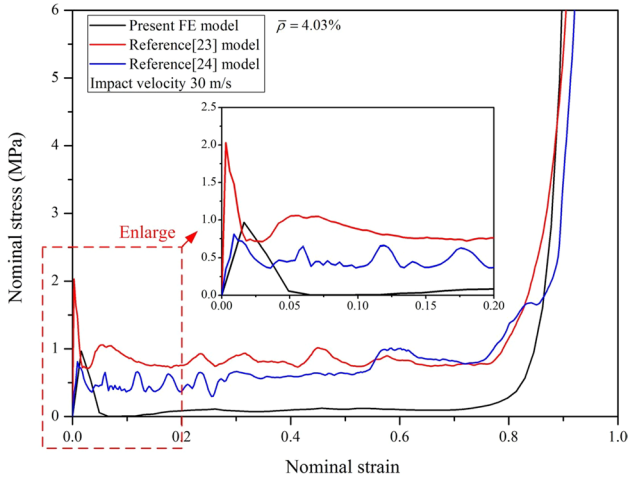

Fig. 4 Nominal stress–strain *curves* of three FE foam models

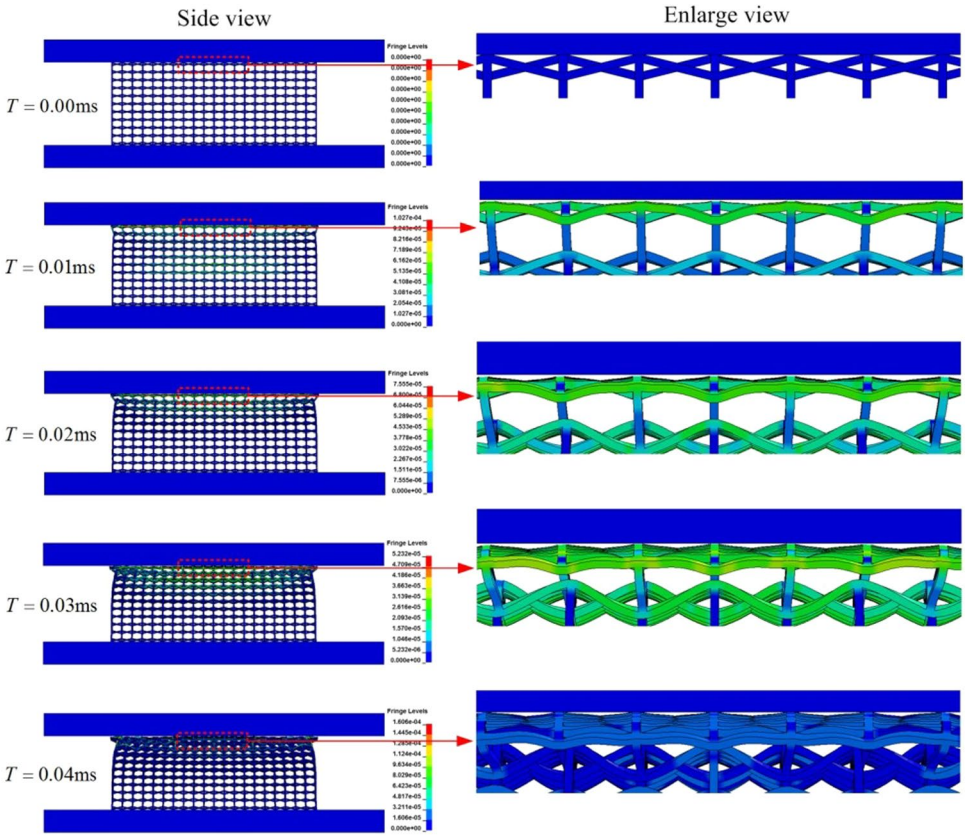

Fig. 5 Deformation process of NPR foam model in the early stage

4.2 Mean plateau stress

McFarland [25] derived a semi-empirical formula to calculate the mean crushing strength of honeycomb structures under axial compression in their pioneer work. Yang [26] investigated experimentally and numerically the uniaxial crushing behavior of aluminum honeycombs in the out-of plane directions. They proposed two semi-empirical equations to determine the crushing strength of honeycombs.

Lu [27] defined mean plateau force as the average values between ε_0 and ε_d. The global maximum of the efficiency curve is used to determine ε_d for hardening/softening behavior. In addition, the last local maximum of the efficiency curve is used to determine ε_d for perfectly plastic behavior [28]. This method has been used in [23, 24] to decide the plateau stress of aluminum foam. A typical stress–strain curve can be seen in Fig. 6, which is obtained from the impact side of FE model under a certain crushing velocity. It is clearly seen that the curve consisted of a linear elastic region, an initial yield point (peak point), a "plateau", and a densification region.

$$\eta(\varepsilon) = \frac{1}{\sigma(\varepsilon)} \int_0^{\varepsilon} \sigma(\varepsilon) \mathrm{d}\varepsilon \tag{2}$$

$$\left. \frac{\mathrm{d}\eta(\varepsilon)}{d\varepsilon} \right|_{\varepsilon=\varepsilon_d} = 0 \tag{3}$$

$$\sigma_{\mathrm{pl}} = \frac{1}{\varepsilon_d - \varepsilon_0} \int_{\varepsilon_0}^{\varepsilon_d} \sigma(\varepsilon) \mathrm{d}\varepsilon. \tag{4}$$

The relationship between plateau stress and impact velocity is depicted in Fig. 7. It could be found that the plateau stress increases with the impact velocity increasing for three relative densities, which is similar with the conclusion of [23, 24]. For the aluminum foam with relative density of 4.03%, when the impact velocity increased from

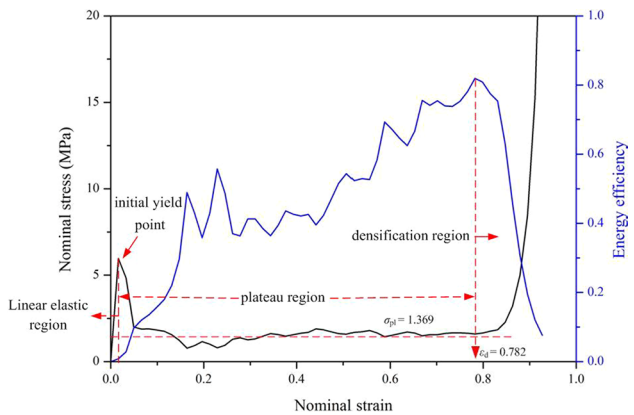

Fig. 6 Dynamic nominal stress–strain curve and the corresponding energy absorption efficiency–strain curve

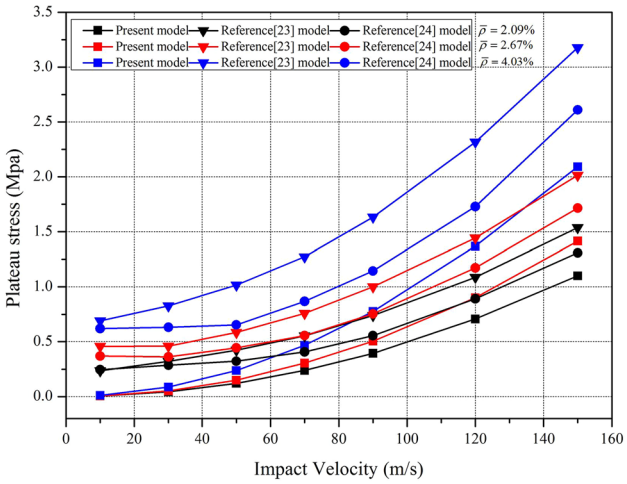

Fig. 7 Effect of impact velocity on proximal end plateau stress

10 to 150 m/s, the plateau stress of present model change from 0.011 to 2.092 MPa enhanced with 189 times, the plateau stress of reference [23] model change from 0.69 to 3.18 MPa enhanced with 3.61 times and the plateau stress of reference [24] model change from 0.62 to 2.61 MPa enhanced with 3.21 times. But which should be noticed that the plateau stress of present model under impact loading is less than the reference [23, 24] model due to the negative Poisson's ratio. In addition, the plateau stress of three relative densities under lower impact velocity in this study is very small and the values are very close, but the difference of plateau stress value has become increasingly obvious with impact velocity increasing. This could be interpreted as the deformation modes of the open-cell aluminum foam with negative Poisson's ratio under impact loading is similar with the conventional aluminum foam, and the negative Poisson's ratio could be considered as an imperfection.

The relative density has a significant effect on the plateau stress of aluminum foam. Figure 8 depicts the effect of relative density on plateau stress under different impact velocities. It can be found that the plateau stress of three models under impact loading increases with the relative density increasing. It can be explained as the integral strength and stiffness of foam enhance and then the plateau stress increases. What is noteworthy is that the increment rate of three models is different due to the different topological micro-structure configurations and the increment rate of present model under different impact velocities increases distinctly with the impact velocity increasing, which the reference [23, 24] model is very close to each others. When the impact velocity increased from 10 to 150 m/s, the slope of the present model curves changes from 0.346 to 51.14 enhanced with 147 times, the slope of the reference [23] model curves changes from 23.50 to 84.56 enhanced with 2.60 times, and the slope of the

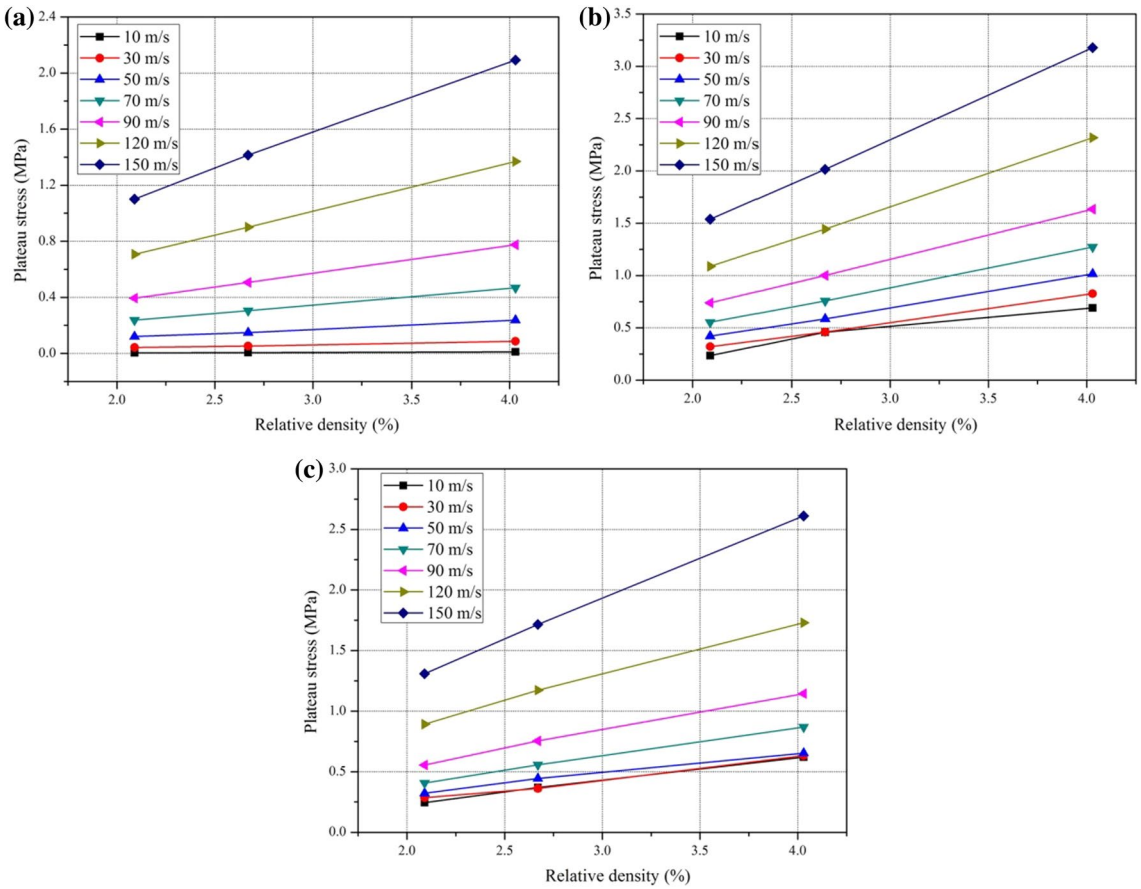

Fig. 8 Effect of relative density on plateau stress at proximal end. **a** Present model. **b** Reference [23] model. **c** Reference [24] model

reference [24] model curves changes from 19.29 to 67.12 enhanced with 2.48 times. It is interesting to note that the loading plateau stress is insensitive to relative density at low loading speeds, while it is significantly increased by increasing relative density at high impact velocities. The former is distinct from the conventional foams as compared in Fig. 8, while the latter is qualitatively consistent with the conventional foams. The reasonable explain is that the deformation process of this NPR foam is different from the conventional foam at low loading speeds. The NPR foam is less stiff than the conventional foam. This indicates that a different mechanism is operating for the NPR foam in response to low-velocity impacts, which is attributed to the plastic hinge formation of cell ribs. There is a temporary separation between the impact plate and the NPR foam due to the bending, torsion, and buckling of cell ribs. However, the inertial force, which is determined by mass or density, contributes much to the loading stress, and thus the loading plateau stress is more sensitive to relative density at higher impact velocities, regardless of the cell structures.

4.3 The specific energy absorption

The specific energy absorption is defined as the ratio of the absorbed energy to the mass of the structure, which could be calculated by the following:

$$\mathrm{SEA} = \frac{E}{m} = \frac{\int_0^{\delta} P d\delta}{m} \tag{5}$$

where E and m are the total energy absorbed during crush and the mass of the specimen, respectively.

Energy absorbed by foams is the area under the force–displacement. The total energy dissipated by three types of foam specimens is calculated to a strain of 0.5 prior to the densification at different conditions.

The specific energy is defined as the energy per unit mass, which could be calculated by Eq. (5). SEA is a suitable parameter to compare the energy absorption capacity of different specimens. The mass of three types of aluminum foam specimens is 3.998×10^{-2} g, 3.626×10^{-2} g, and 3.254×10^{-2} g for aluminum foams with cell height $h=1$ mm, $h=0.75$ mm and $h=0.5$ mm, respectively.

The impact loading applied to specimens varies under different impact velocities. Thus, SEA is a suitable parameter for comparing the energy absorption capacity. Figure 9 shows the changes in the SEA of three models under seven impact velocities that range from 10 to 150 m/s. These numerical results indicate that the SEA and the growth rate gradually increase when the impact velocity increases. Moreover, no linear relationship was found between SEA and the impact velocity. What is noticed that the SEA of present model is lower than the reference [23, 24] model under low impact velocity, and the metal hollow sphere foam model [24] is higher than present model but lower than the 14-sided polyhedron model [23].

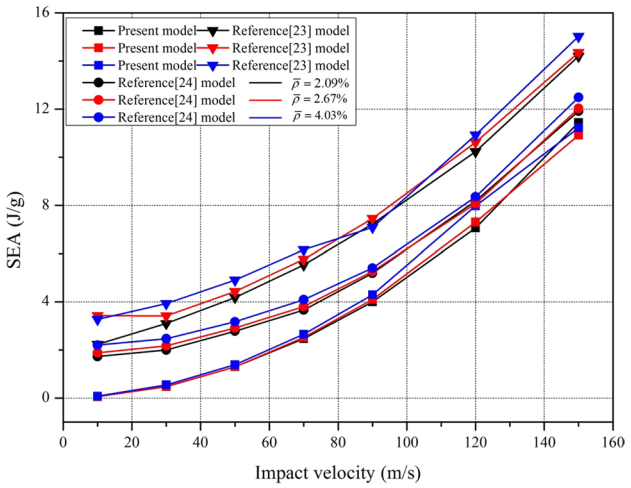

Fig. 9 Impact velocities effect on SEA of three different foam FE models

Three relative densities and seven impact velocities are used to investigate the effect of relative density on SEA of different model, as shown in Fig. 10. It can be found that the SEA of three models almost increases linearly with the relative density increasing. The slope of present model curves is very small under lower impact velocity; however, the slope increases progressively with the impact velocity increasing when the impact velocity reached 90 m/s. These numerical results indicated that the open-cell foam with negative Poisson's ratio is not suitable for energy absorption under low-velocity impact due to the lower SEA and lower growth ratio with relative density increasing.

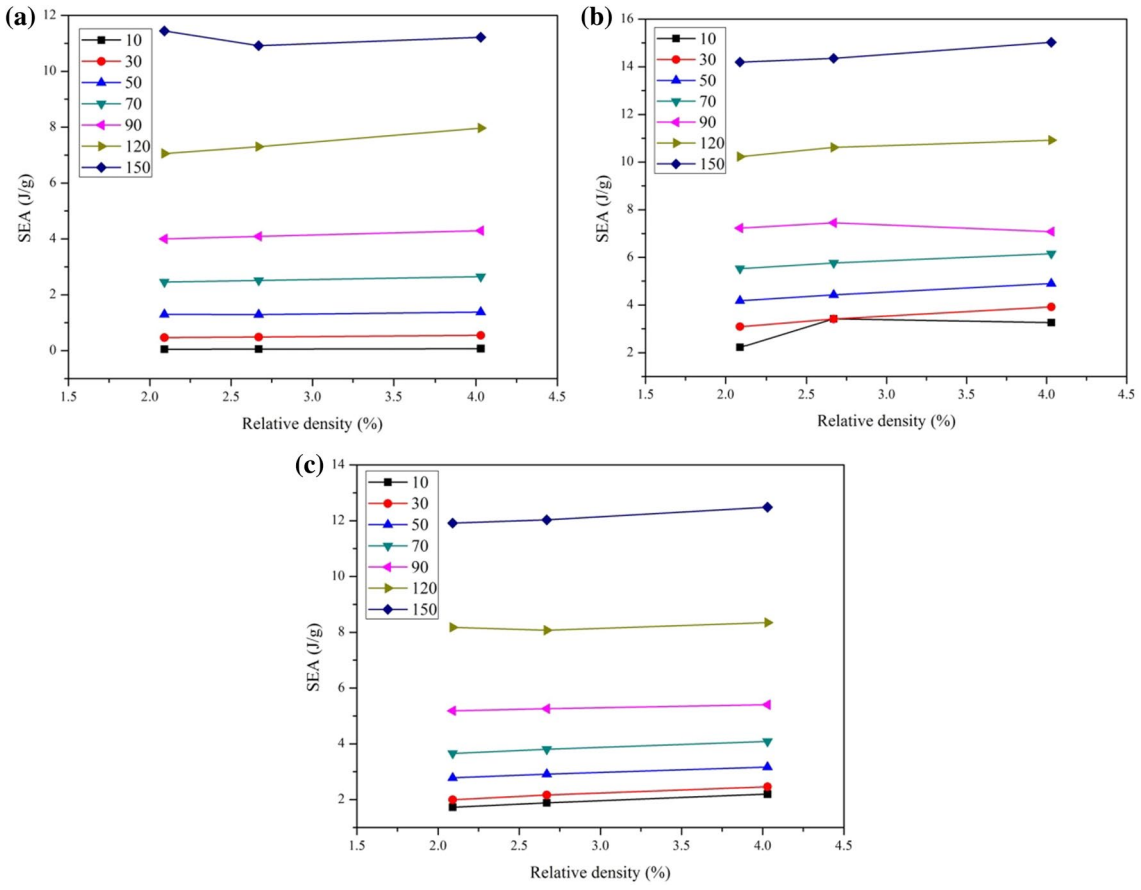

Fig. 10 Effect of relative densities on the SEA with different impact velocities. **a** Present model. **b** Reference [23] model. **c** Reference [24] model

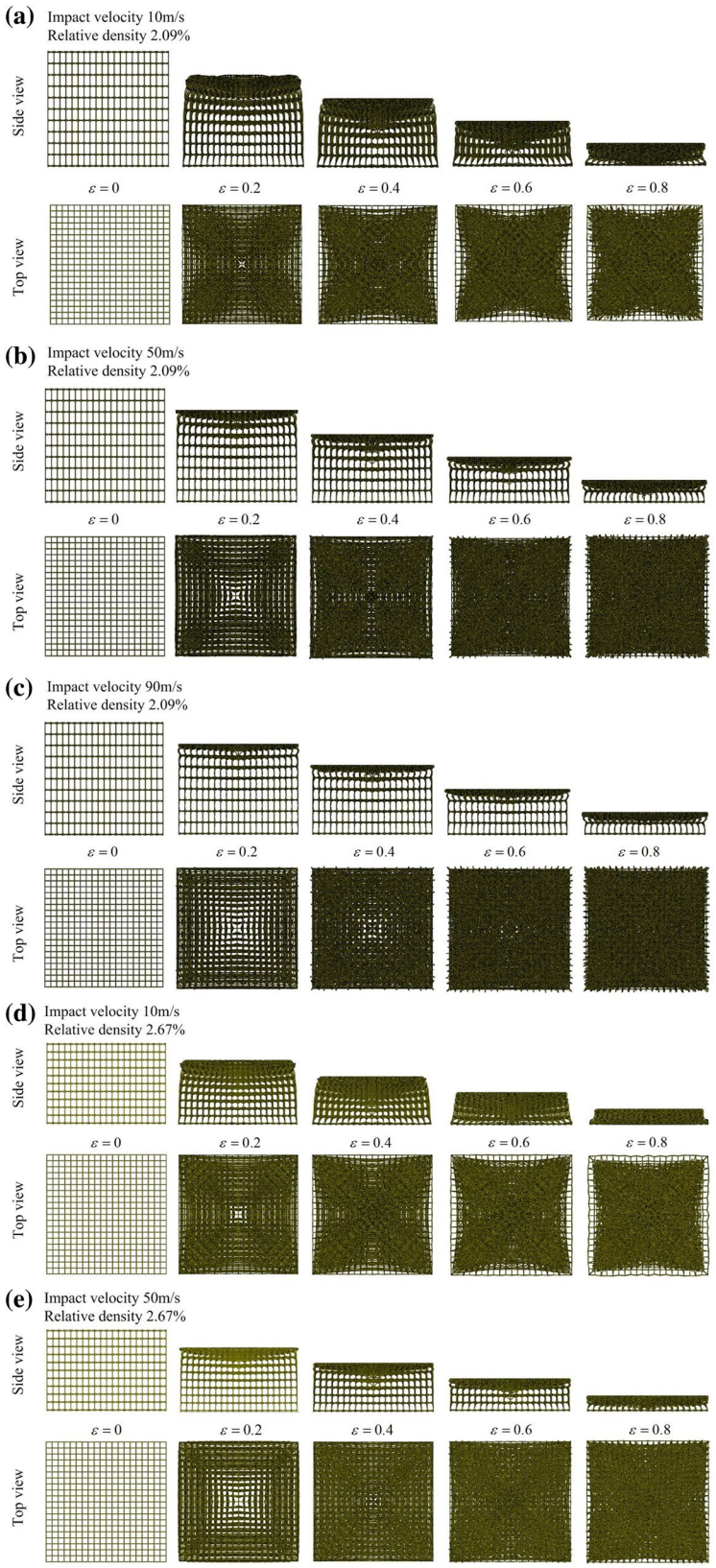

Fig. 11 Deformation process of NPR foams with different relative densities under different impact velocities: **a** $\bar{\rho} = 2.09\%, v = 10$m/s, **b** $\bar{\rho} = 2.09\%, v = 50$m/s, **c** $\bar{\rho} = 2.09\%, v = 90$m/s, **d** $\bar{\rho} = 2.67\%, v = 10$m/s, **e** $\bar{\rho} = 2.67\%, v = 50$m/s, **f** $\bar{\rho} = 2.67\%, v = 90$m/s, **g** $\bar{\rho} = 4.03\%, v = 10$m/s, **h** $\bar{\rho} = 4.03\%, v = 50$m/s, and **i** $\bar{\rho} = 4.03\%, v = 90$m/s

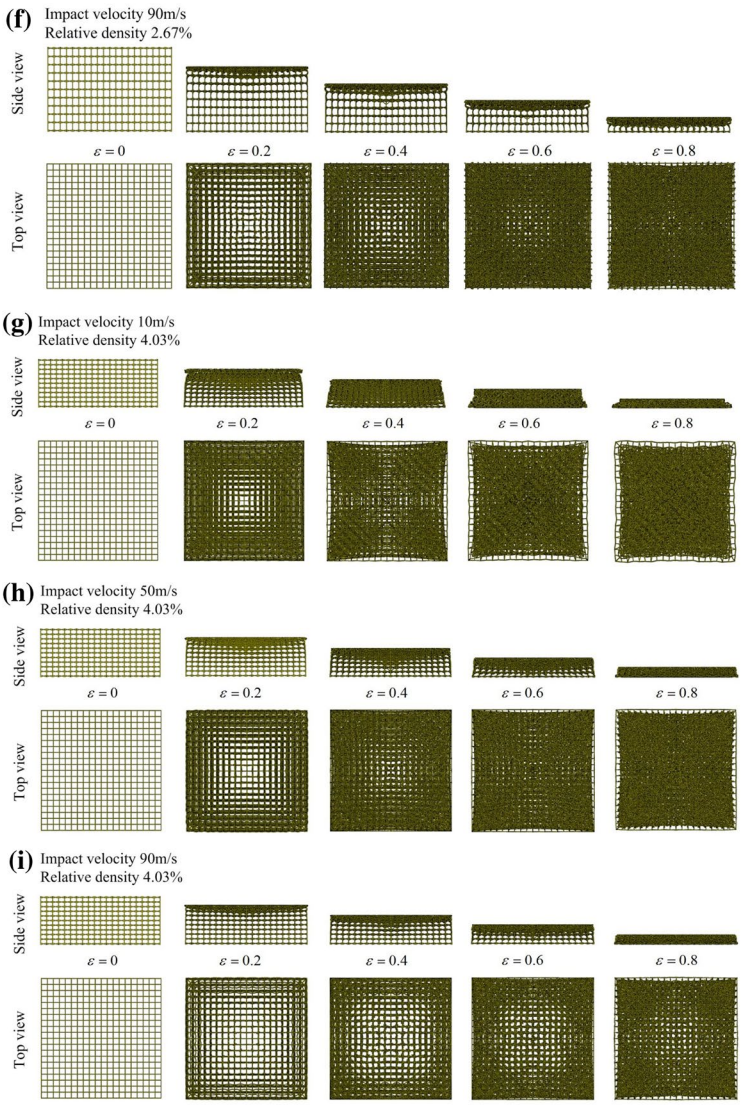

Fig. 11 (continued)

4.4 Deformation mechanism

Deformation mode has a direct relation of the material properties and its geometry topology of micro-structure. It will also display diverse deformation under different impact velocities. Figure 11 displays the detail deformation process under three different impact velocities and relative densities. Figure 11a–c shows the negative Poisson's ratio open-cell foam with relative density 2.09% deformation process under three different impact velocities 10, 50, and 90 m/s. It is seen from Fig. 11a that the dominant deformation of foam is overall deformation and the lattices shrink progressively from edge to center in other two no load directions due to the negative Poisson's ratios in bilateral directions. The overall deformation under 50 m/s is not the dominant mode which is convert to localized compression and is different from the deformation pattern observed at 10 m/s, as shown in Fig. 11b. The loading direction deformation occurs first at the proximal end and then propagates downward gradually. The magnitude of the localized deformation is larger in the top contact region than that in center region, which indicated that the inertia force during the accelerating process caused obvious deformation in the specimen. Obvious crush band is observed at impact velocity 50 m/s which is different from the deformation pattern at impact velocity 10 m/s. It is indicated that the negative Poisson's ratio effect becomes smaller with the impact velocity increasing. The deformation starts from the proximal end of the specimen and then propagates to the distal end under impact velocity 90 m/s, which is similar to the deformation pattern observed at impact velocity 50 m/s, as shown in Fig. 11c. The deformation is nearly un-deformation in the distal region of the specimen when the impact velocity exceeds the 90 m/s. Thus, the localized crush band is observed at all impact velocity in this study.

Figure 11a, d, g shows the effect of relative density on deformation modes under the same impact velocity. Overall deformation is also the dominant deformation of all relative density; however, the overall deformation is more and more obvious with the relative density increasing due to the height of specimen decreasing. It was suggested that the impact velocity was the major factor that influenced the deformation modes of the cellular material. Based on the numerical simulation consequences, the dominant deformation of foam was overall deformation when the impact velocity was low. And when the velocity is sufficiently high, the crushing bands are highly localized at the impact side, which is the progressive mode deformation in usual, and then propagate along the impact direction. Figure 11d–f, g–i shows the negative Poisson's ratio open-cell foam with relative density 2.67 and 4.03% deformation process under three different impact velocities 10, 50, and 90 m/s, respectively. It could be obtain that the deformation processes of these higher relative density foams are very similar with that of NPR foam with relative density 2.09%. However, it is notable that the effect of NPR becomes more and more apparent with the relative density increasing when the strain exceeds 0.4, although the plateau stress is not improving much at low loading speeds. Under high impact velocity, the compression started from the impact side and then propagated to the distal end regardless of the cell structures. This deformation process is similar with that of NPR foam with relative density 2.09%. It can be concluded that the length-to-height ratio which is defined for a cell having certain geometric characteristics is a key parameter to design the NPR foams materials, and the bigger of the ratio the more obvious of this phenomenon in some geometry configurations at low loading speeds.

5 Summary

The dynamic crushing behavior of three kinds of open-cell aluminum foams with different relative densities is numerically investigated. The influence of impact velocity and relative density on plateau stress, SEA, and deformation modes is discussed. The following conclusions can be drawn from the results and discussions.

The simulation results indicate that the inertia effect of NPR open-cell foam material is obvious at the proximal end. The plateau stress and SEA of NPR open-cell foam under impact loading are less than the conventional foam with the same relative density. The NPR open-cell foam material is not suitable for energy absorption under low-velocity impact. The deformation pattern of NPR open-cell foam material is completely different from the conventional foam material under impact loading due to the negative Poisson's ratio properties. The negative Poisson's ratio effect on deformation modes becomes smaller with the impact velocity increasing. The length-to-height ratio is a key parameter to design the NPR foams materials to behave its nature properties.

Acknowledgements This work is supported by the National Natural Science Foundation of China (Grant Nos.11572214, 11402163), Natural Science Foundation of Shanxi Province (Grant No. 2013011005-2), Shanxi Scholarship Council of China (2013-046), and the Top Young Academic Leaders of Shanxi and the Outstanding Innovative Teams of Higher Learning Institutions of Shanxi. The financial contributions are gratefully acknowledged.

References

1. G. Lu, T.X. Yu Energy Absorption of Structures and Materials. (Wood head Publishing Ltd., Cambridge, 2003)
2. L. Jing, Z.H. Wang, J.G. Ning et al., The dynamic response of sandwich beams with open-cell metal foam cores. Compos. Part B **42**(1), 1–10 (2011)
3. L. Jing, Z.H. Wang, L.M. Zhao, Dynamic response of cylindrical sandwich shells with metallic foam cores under blast loading—numerical simulations. Compos. Struct **99**, 213–223 (2013)
4. L.J. Gibson, M.F. Ashby, Cellular Solids. Structure and Properties (Press Syndicate of the University of Cambridge, Cambridge, 1997)
5. M.F. Ashby, A.G. Evans, N.A. Fleck et al., Metal Foams: A Design Guide (Butter worth–Heinemann, Oxford, 2000)
6. H. Yu, Z. Guo, B. Li et al., Research into the effect of cell diameter of aluminum foam on its compressive and energy absorption properties. Mater. Sci. Eng. A **454–455**(16), 542–546 (2007)
7. V.H. Carneiro, J. Meireles, H. Puga, Auxetic materials—a review. Mater. Sci-Poland **31**, 561–571 (2013)
8. M. Ruzzene, F. Scarpa, F. Soranna, Wave beaming effects in two-dimensional cellular structures. Smart. Mater. Struct **12**, 363 (2003)
9. F. Scarpa, Auxetic materials for bioprostheses. IEEE Signal Process. Mag. **25**(5), 126–128 (2008)
10. J.B. Choi, R.S. Lakes, Design of a fastener based on negative Poisson's ratio foam. Cell Polym. **10**, 205–212 (1991)
11. Y. Sun, N. Pugno, Hierarchical fibers with a negative Poisson's ratio for tougher composites. Materials **6**(2), 699–712 (2013)
12. Y.J. Park, J.K. Kim, The effect of negative Poisson's ratio polyurethane scaffolds for articular cartilage tissue engineering applications. Adv. Mater. Sci. Eng. **2013** (2013). doi:10.1155/2013/85289
13. Q. Liu, Literature Review: Materials with Negative Poisson's Ratios and Potential Applications to Aerospace and Defence (DSTO Defence Science and Technology Organisation, Australia, 2006)
14. Y. Prawoto, Seeing auxetic materials from the mechanics point of view: a structural review on the negative Poisson's ratio. Comp. Mater. Sci. **58**, 140–153 (2012)
15. K.E. Evans, A. Alderson, Auxetic materials: functional materials and structures from lateral thinking. Adv. Mater. **12**, 617 (2000)
16. W. Yang, Z.M. Li, W. Shi et al., Review on auxetic materials. J. Mater. Sci. **39**, 3269–3279 (2004)
17. S. Xu, J.H. Beynon, D. Ruan et al., Experimental study of the out-of-plane dynamic compression of hexagonal honeycombs. Compos. Struct. **94**(8), 2326–2336 (2012)
18. X.L. Gao, An exact elasto-plastic solution for a thick-walled spherical shell of elastic linear-hardening material with finite deformations. Int. J. Pres. Ves. Pip. **57**(1), 45–56 (1994)

19. I. Elnasri, S. Pattofatto, H. Zhao et al., Shock enhancement of cellular structures under impact loading: part I Experiments. J. Mech. Phys. Solids **55**, 2652–2671 (2007)
20. Y. Sun, Q.M. Li, S.A. McDonald et al., Determination of the constitutive relation and critical condition for the shock compression of cellular solids. Mech. Mater. **99**, 26–36 (2016)
21. T.X. Yu, L.L. Hu Mechanical behavior of hexagonal honeycombs under low-velocity impact—theory and simulations. Int. J. Solids Struct. **50**, 3152–3165 (2013)
22. Y. Sun, Q.M. Li, Effect of entrapped gas on the dynamic compressive behaviour of cellular solids. Int. J. Solids Struct. **63**, 50–67 (2015)
23. Z.Q. Li, C.Q. Xi, L. Jing et al., Effect of loading rate on the compressive properties of open-cell metal foams. Mater. Sci. Eng. A **592**, 221–229 (2014)
24. J.H. Fan, J.J. Zhang, Z.H. Wang et al., Dynamic crushing behavior of random and functionally graded metal hollow sphere foams. Mater. Sci. Eng. A **561**, 352–361 (2013)
25. R.K. Mc Farland, Hexagonal cell structures under post-buckling axial load. J. Am. Inst. Aeronaut. Astronaut. **1**(6), 1380–1385 (1963)
26. M. Yang, P. Qiao, Quasi-static crushing behavior of aluminum honeycomb materials. J. Sandwich Struct. Mater. **10**(2), 133–160 (2008)
27. A.S.M. Ashab, D. Ruan, G. Lu et al., Experimental investigation of the mechanical behavior of aluminum honeycombs under quasi-static and dynamic indentation. Mater. Des. **74**, 138–149 (2015)
28. Q.M. Li, I. Magkiriadis, J.J. Harrigan, Compressive strain at the onset of densification of cellular solids J. Cell. Plast. **42**, 371–392 (2006)